Validity of timedependent selfconsistentfield (TDSCF) approximations for unimolecular dynamics: A test for photodissociation of the Xe–HI cluster

R. Alimi, R. B. Gerber, A. D. Hammerich, R. Kosloff, and M. A. Ratner

Citation: The Journal of Chemical Physics **93**, 6484 (1990); doi: 10.1063/1.458965
View online: http://dx.doi.org/10.1063/1.458965
View Table of Contents: http://scitation.aip.org/content/aip/journal/jcp/93/9?ver=pdfcov
Published by the AIP Publishing

Validity of time-dependent self-consistent-field (TDSCF) approximations for unimolecular dynamics: A test for photodissociation of the Xe–HI cluster

R. Alimi
Department of Physical Chemistry and The Fritz Haber Center for Molecular Dynamics, The Hebrew University of Jerusalem, Jerusalem 91904, Israel

R. B. Gerber
Department of Physical Chemistry and The Fritz Haber Center for Molecular Dynamics, The Hebrew University of Jerusalem, Jerusalem 91904, Israel and Department of Chemistry, University of California, Irvine, California 92717

A. D. Hammerich and R. Kosloff
Department of Physical Chemistry and The Fritz Haber Center for Molecular Dynamics, The Hebrew University of Jerusalem, Jerusalem 91904, Israel

M. A. Ratner
Department of Chemistry, Northwestern University, Evanston, Illinois 60208

(Received 18 December 1989; accepted 11 July 1990)

The photodissociation dynamics of a collinear model of the van der Waals cluster Xe–HI is used as a testing ground for time-dependent self-consistent field (TDSCF) approximations. In this study, the quantum-mechanical TDSCF and a combined classical/quantal TDSCF (in which the light atom is treated quantum mechanically, the heavy atoms are treated classically) are compared to numerically exact wave packet calculations. Very good agreement is found between the TDSCF approximations and the exact result over the entire subpicosecond time duration of the process. In particular, all the properties related to the quantal degree of freedom in the combined quantal/classical TDSCF method reproduce almost perfectly the exact results. However, the classical mode in the hybrid approximation is somewhat less well described due to insufficient representation of energy transfer between the modes. The conclusions are very promising as to the applicability of TDSCF methods, in particular the hybrid quantal/classical scheme to more complex systems in which only a few degrees of freedom can be treated quantum mechanically.

I. INTRODUCTION

Obtaining the detailed evolution in time of fundamental molecular processes is an important challenge for theory in the field of molecular reaction dynamics. Rigorous, numerically exact calculations are at present feasible only for the simplest systems. For instance, the pseudospectral method, based on the fast Fourier transform (FFT) algorithm, is a powerful method for dealing with the time-dependent Schrödinger equation.[1,2] The method is accurate and easily implemented, but it is practically limited at present to systems having a small number of degrees of freedom due to the exponential increase of computational time and effort with dimensionality. Moreover, the method becomes prohibitively expensive when one or more of the degrees of freedom approach the classical limit (e.g., heavy particles, high energy).

Progress in time-dependent studies of molecular systems depends, therefore, to a large extent on the development of approximate methods. Among the important approximations available are the time-dependent self-consistent field (TDSCF) methods. These methods have their origins in the earliest years of quantum theory,[3] but only in recent years have these methods been adapted and applied to problems in molecular dynamics, including unimolecular dynamics and dissociation,[4–6,11] molecular scattering,[7,33] and several other topics.[8–10]

There are, in fact, several different TDSCF approximations, although they are closely related. In the quantal TDSCF method, originally due to Dirac,[3] each mode is described by a time-dependent wave function governed by a one-dimensional Schrödinger equation. The effective potential in the TDSCF equations for any single mode is time dependent, and represents an average field due to all the other modes. The TDSCF approach which has had the widest use in molecular dynamics employs a mixed quantum-mechanical/classical treatment.[4–8] In this scheme some of the modes (e.g., a light atom) are described quantum mechanically, while the other modes are treated classically. The TDSCF method derives equations that include mutual coupling between the quantum and the classical subsystems. We refer to this scheme as the quantum/classical TDSCF (Q/C TDSCF).

Although the TDSCF methods, in particular the Q/C TDSCF, have been applied in a fair number of studies in recent years, these approximations have generally not been tested against rigorous calculations. Indeed, to our knowledge there have been only two tests of quantum TDSCF by Kosloff *et al.* One[11] was for vibrational predissociation in a collinear model of I_2He, which is a weak coupling system (relatively inefficient energy transfer between the I_2 vibration and the van der Waals mode). The other[34] employed a

 0021-9606/90/216484-07$03.00

model system to compare TDSCF and multiconfigurational TSDCF approximations with the numerically exact simulations for the dynamics of curve crossing processes subject to coupling to a heat bath. It is clearly desirable to provide more tests of the TDSCF approximations for other types of processes.

The purpose of the present study is to test both the quantum TDSCF and the hybrid Q/C TDSCF for a direct photodissociation process in a collinear model of the van der Waals cluster Xe(HI), following electronic excitation of the HI molecule into a repulsive state. There has been considerable interest in photoinduced chemical reactions in van der Waals clusters,[12–14] which is part of our motivation for choosing a process of this type. Hydrogen–halide/rare gas clusters have been extensively pursued, both experimentally[15–17] and theoretically[18,19] hence we consider a model of such a system.

Moreover, recently all-modes full 3D calculations were carried out for photodissociation of HI in the clusters Xe_n(HI), for n in the range 1 to 12[20] and also for photodissociation of HI in solid Xe.[20,21] These calculations were carried out both using classical molecular dynamics simulations[21] and using the hybrid Q/C TDSCF.[20] The accuracy of the Q/C TDSCF for systems and processes of this type is thus a very pertinent question. The restriction to a collinear model in the present study was made to simplify the exact numerical solution of the time-dependent Schrödinger equation implemented by the FFT grid method,[1,2] which serves as the reference for testing the quantum TDSCF and the Q/C TDSCF.

The outline of the article is as follows. Section II describes the model system used. Section III outlines the quantum TDSCF and the Q/C TDSCF methods and describes the numerical algorithms used. The results are given in Sec. IV. The conclusions are discussed in Sec. V.

II. MODEL AND POTENTIAL FUNCTIONS

A. The system and the process

This study explores the photodissociation dynamics of the Xe(HI) cluster. The photolytic process to which we refer results from electronically exciting the HI molecule within the cluster from its ground state $^1\Sigma^+$ to the purely excited state $^1\Pi$. Studies of several clusters of the type MHX, where X is a halide and M a rare-gas atom have been reported in the literature.[15–19] In all these cases the electronic ground state equilibrium configuration is collinear, with H pointing towards the rare-gas atom.[15–19] We assume the same holds for XeHI, which has not been reported yet. Although collinear Xe–HI is most likely the correct classical equilibrium structure, restriction of the description of the dynamics to a collinear framework is certainly a drastic simplification that cannot do justice to the real physics of the problem. This is obvious from the large bending amplitudes of the MHX clusters.[15–19] The collinear assumption must, therefore, be thought of as a very simplistic model, adopted only because of the computational effort required to solve the time-dependent Schrödinger equation exactly for more than 2 degrees of freedom.

B. The coordinate system

The choice of the coordinate system is a key issue in self-consistent field approximations.[22] SCF treatments involve a kind of formal mutual separation of coordinates, and the results of the approximation depend on the choice of modes. It has been found in time-dependent SCF studies that significant improvements in the approximation can be made by a judicious choice of the coordinates that are being mutually factorized (in the SCF sense).[23] Recently efforts were made to optimize coordinates in TDSCF calculations, although so far only in the framework of Cartesian modes.[24]

The motivation for the choice of the coordinates in our system is twofold. First, it is more convenient to choose a reference frame in which the kinetic energy operator is diagonal, hence the coupling between the modes is purely potential. Second, the coordinates should be convenient for integration of the equations of motion in the TDSCF framework.

These considerations led us to choose a Jacobi set of coordinates r and R described in Fig. 1. R is the distance between Xe and the center of mass of HI and r is the interatomic HI separation. Although the center of mass of HI lies essentially on the iodine atom, choosing R as the Xe–I distance would not diagonalize the kinetic energy operator. Moreover, the "quantum particle," the hydrogen atom, is accurately described by the motion in r while the two heavy particles Xe and I, which are more likely to behave classically, depend only on R.

This choice of coordinates is not unique. Unlike the exact solution which is independent of the particular reference frame, approximate solutions such as TDSCF can be very sensitive to it. In the present work the coordinate system was not varied. The coordinates used may well not be the optimal ones for the TDSCF approximations, however, the excellent agreement between the exact and the approximate solutions justifies the validity of our choice *a posteriori*.

C. Interaction potentials

To represent the initial state for the process we assume a vertical transition from the collinear ground state to a dissociative excited state. The potential surface for this excited state is modeled as a sum of three terms, i.e., the surface is taken as a sum of pairwise interactions between the atoms involved

$$V(r,R) = V_{\text{H-I}}(r) + V_{\text{H-Xe}(R-r+\delta)} + V_{\text{Xe-I}}(R+\delta). \quad (1)$$

In Eq. (1) δ is the difference between the HI center of mass

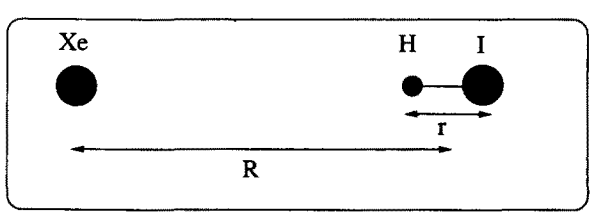

FIG. 1. Coordinate system for the collinear model Xe–HI.

position and the iodine position, and the coordinates r and R are defined above. Because of the magnitude of the reduced mass μ_{HI}, δ is on the order of 10^{-2} Å and therefore can be neglected for the calculation of the potential, hence

$$V(r,R) \approx V_{H\text{-}I}(r) + V_{H\text{-}Xe}(R-r) + V_{Xe\text{-}I}(R). \quad (2)$$

The HI pair potential is chosen to fit the excited repulsive $^1\Pi$ state,[25]

$$V_{H\text{-}I}(r) = Ae^{-\alpha r}, \quad (3)$$

where $A = 34.24$ eV, $\alpha = 1.934$ Å^{-1}.
The Xe–I potential is given by

$$V_{Xe\text{-}I}(R) = Be^{-\beta R} - \frac{C}{R^6} \quad (4)$$

with $B = 599.99$ eV, $\beta = 2.614\,19$ Å^{-1}, and $C = 534.5199$ eV Å^6. These three parameters are adjusted in order to fit the more elaborate potential form of Casavecchia *et al.*[26] The H–Xe coupling term is given by

$$V_{H\text{-}Xe}(R-r) = \frac{\epsilon}{\alpha - 6} \times \left[6e^{\alpha[1-(R-r/r_m)]} - \alpha\left(\frac{r_m}{R-r}\right)^6\right], \quad (5)$$

where $\epsilon = 6.81$ meV, $r_m = 3.95$ Å, $\alpha = 14.28$, obtained from scattering data.[27]

III. METHODS

A. Exact propagation scheme

The quantum propagation dynamics of the system are described by the time-dependent Schrödinger equation

$$i\hbar \frac{\partial \Psi(r,R,t)}{\partial t} = \hat{\mathbf{H}}\Psi(r,R,t), \quad (6)$$

where $\hat{\mathbf{H}}$ is the quantum Hamiltonian of the system.

$$\hat{\mathbf{H}} = \hat{\mathbf{T}} + \hat{\mathbf{V}} = \frac{\hat{\mathbf{p}}_r^2}{2\mu_r} + \frac{\hat{\mathbf{p}}_R^2}{2\mu_R} + \hat{V}(r,R). \quad (7)$$

The reduced masses are given by

$$\mu_r = \frac{m_H m_I}{m_H + m_I}, \quad \mu_R = \frac{m_{Xe}(m_I + m_H)}{m_H + m_I + m_{Xe}} \quad (8)$$

and the potential operator $\hat{\mathbf{V}}$ is described above.

We solved the time-dependent Schrödinger equation by the wave packet grid method developed by Kosloff.[1,2] The wave function is represented on a two-dimensional rectangular grid, on which one calculates the Hamiltonian operations locally. The potential is a local operator therefore the simple multiplication of V by Ψ point by point gives the result. For the kinetic energy operator a two dimensional Fourier transform is performed. In momentum space, $\hat{\mathbf{T}}$ is local and results from the multiplication of $\Psi(k)$, the Fourier transform of the configuration space wave function, by k^2 for each degree of freedom. An inverse Fourier transform takes the wave function back into the space coordinates. For the time evolution, we used a Chebychev polynomial scheme.[28] The time propagation operator is expressed as

$$\hat{\mathbf{U}}(t) = e^{-i\hat{\mathbf{H}}t/\hbar} = \sum_{n=0}^{N} a_n \phi_n(-i\hat{\mathbf{H}}_{norm}), \quad (9)$$

where ϕ_n is the complex Chebychev polynomial given by their recursion relations, a_n are expansion coefficients, $\hat{\mathbf{H}}_{norm}$ represents a normalized Hamiltonian where the range of eigenvalues represented on the grid is shifted to the interval $[-1, 1]$. The initial wave function $\Psi(r,R,0)$ is expressed as a product of two Gaussians, respectively, centered on r_{eq} and R_{eq}. These are taken as the equilibrium values of r_{HI}, R_{XeI} in the electronic ground state of the XeHI complex:

$$\Psi(r,R,0) = \Psi_1(r)\Psi_2(R). \quad (10)$$

B. Quantum TDSCF and Q/C TDSCF

The time-dependent wave function of the system is assumed to be separable.[5,22]

$$\Psi(r,R,t) = \Psi_1(r,t)\Psi_2(R,t)e^{[i\gamma(t)]} \quad (11)$$

The factor $e^{[i\gamma(t)]}$ is of no importance for our purpose and will not be discussed further.[5,22] Substituting Eq. (11) in Eq. (6) one gets

$$\left[\frac{-\hbar^2}{2\mu_r}\nabla_r^2 + V_1^{eff}(r,t)\right]\Psi_1(r,t) = i\hbar\frac{\partial\Psi_1(r,t)}{\partial t}, \quad (12a)$$

$$\left[\frac{-\hbar^2}{2\mu_R}\nabla_R^2 + V_2^{eff}(R,t)\right]\Psi_2(R,t) = i\hbar\frac{\partial\Psi_2(R,t)}{\partial t}. \quad (12b)$$

These are the quantum mechanical TDSCF equations for the system, where

$$V_1^{eff}(r,t) = \langle\Psi_2(R,t)|V(r,R)|\Psi_2(R,t)\rangle_R \quad (13a)$$

and

$$V_2^{eff}(R,t) = \langle\Psi_1(r,t)|V(r,R)|\Psi_1(r,t)\rangle_r. \quad (13b)$$

The time dependence of the effective potential allows energy flow between modes. It is possible to solve the above equations as described in Ref. 11. These are the quantum TDSCF equations. The mixed quantum/classical scheme, the Q/C scheme, and its derivation are discussed in Refs. 5 and 22. For the present purpose it is most easily obtained by taking the classical limit of the equation for the R mode. This gives

$$\dot{p}_R = -\frac{\partial V_2^{eff}}{\partial R}, \quad (14a)$$

$$\dot{R} = \frac{p_R}{\mu_R}, \quad (14b)$$

where V_2^{eff} is defined in Eq. (13.b).

The mean field acting on the r mode becomes

$$V_1^{eff} = \frac{1}{n_T}\sum_{\alpha=1}^{n_T} V[r,R_\alpha(t)], \quad (15)$$

where α labels the various initial values sampling the different initial conditions for the n_T classical trajectories in the R mode. Hamilton's equations (14) are solved by the variable order and variable time step Adams–Moulton predictor corrector method. The remaining quantum TDSCF equation (12.a) is solved using the same procedure as in the exact propagation scheme. Even though the Hamiltonian is time dependent it is still possible to use a Chebychev polynomial expansion. Usually in these cases one has to use second order differencing (SOD).[29] for instance, in the quantum TDSCF

approximation, the time propagation is done simultaneously in the two modes by the SOD scheme

$$\Psi_{1,2}(t+\Delta t) = \Psi_{1,2}(t-\Delta t) - 2i\Delta t\hat{H}_{\rm SCF}\Psi_{1,2}(t), \qquad (16)$$

where Δt is typically of the order of 1 a.u. However, even if $\hat{H}_{\rm SCF}$ is time dependent, it is still possible to utilize the powerful Chebychev scheme by making the following approximation. Because of the extreme mass ration μ_r/μ_R, during a short period of time, the moving hydrogen senses a nearly static Xe–I configuration. Convergence tests have shown that with time jumps of about 50 a.u. the Chebychev scheme conserves energy and norm. During these jumps R remains unchanged. After each quantum time step, R is recalculated according to Eqs. (14). This procedure is computationally preferable to the SOD propagation scheme.

C. Computational considerations

The main advantage of the TDSCF approximations, beside their easy implementation, relies on the important gain of computational time and memory storage. All the calculations reported in this paper have been done on a CCI computer with a single scalar processor peaking at 10 MIPS. The relative computational times (CPU) are the following:

Q/C TDSCF:*Q TDSCF*: exact = 1:40:60.

Both the Q/C TDSCF and the exact methods use the global Chebychev propagator while the Q TDSCF uses the SOD scheme. This explains the poor ratio 40:60 between the quantum TDSCF and the exact calculations. The relative memory requirements are approximately the following:

Q/C TDSCF: *Q TDSCF*: exact = 1:2:50.

As one sees, both considerable time and memory saving are provided by the hybrid Q/C TDSCF approximation. These gains are expected to increase very steeply with the number of degrees of freedom of the system. The Q/C TDSCF and the Q TDSCF thus make it possible to treat a wide range of applications for which exact calculations cannot be contemplated at the present stage.

IV. RESULTS

In the exact calculation the initial wave function is taken as the product

$$\Psi(r,R,0) = \Psi_1(r)\Psi_2(R). \qquad (17)$$

The same product is used to describe the initial states for both the quantum and Q/C TDSCF approximation. The narrow initial Gaussian $\Psi_2(R)$ for the classical mode R can be described by five initial conditions. They are chosen at $R_{\rm eq} \pm \Delta R$, $\pm 2\Delta R$ with $\Delta R = 0.1$ Å. We now turn to the description of the results.

In Fig. 2 six "snapshots" at different time points compare the probability amplitude of the exact and the Q/C TDSCF wave function as a function of r, i.e., $|\Psi(r,R,t)|^2$ vs $|\Psi_1(r,t)|^2$. $\Psi_1(r,t)$ is the solution of the TDSCF equation (12a) coupled with the classical equations (14) for the mode R. In this comparison the exact wave function is evaluated for the average value of R at each time t ($\equiv \overline{R}_t$). There is remarkably good agreement between the exact and the approximate solution. The quality of the agreement between

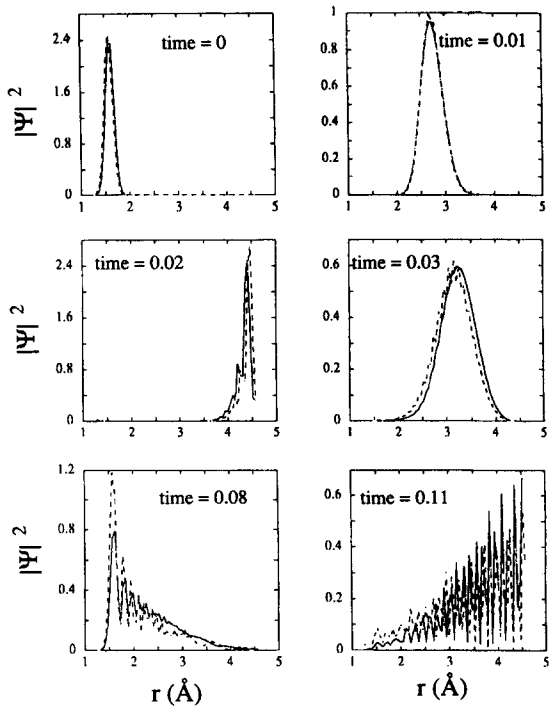

FIG. 2. The probability amplitude as a function of r. The solid line is the exact solution, the dashed line is the Q/C TDSCF.

the approximation and the exact calculation must be judged keeping in mind that the wave function is a highly sensitive quantity (e.g., compared with expectation values). In fact, within the first 0.08 ps the two curves are very close. Beyond 0.08 ps, the peak positions remain the same, but the calculated intensities begin to show a difference. After 0.1 ps the comparison is less straightforward as the wave packet becomes more and more delocalized and structured. Therefore, we need an additional tool for comparing the two wave functions.

Figure 3 shows two different methods of calculating the overlap between the wave functions as a function of time. The dashed line is the usual overlap defined by

$$S_1(t) = |\langle \Psi_{\rm exact}(r,\overline{R}_t,t)|\Psi_{\rm SCF}(r,t)\rangle_r|, \qquad (18)$$

where $\overline{R}_t$ is the current average value of R at time t. The solid line represents the overlap between the moduli of the two

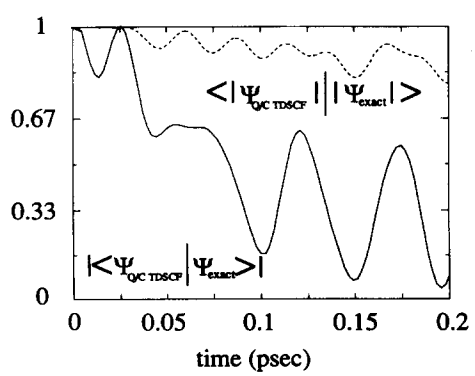

FIG. 3. Two measures of the overlap between the exact solution and the Q/C TDSCF solution, as a function of time. See the text.

states defined by

$$S_2(t) = \langle |\Psi_{\text{exact}}(r,\bar{R}_t,t)|\,|\Psi_{\text{SCF}}(r,t)|\rangle_r. \quad (19)$$

If the agreement between the exact solution and the approximate one were perfect, both S_1 and S_2 should be equal to 1 at any time. $S_1(t)$ and $S_2(t)$ differ basically by a phase term. It is not surprising that S_2 diverges from unity less than S_1. The SCF scheme makes some phase error by considering only mean fields. In general, this implies that better agreement between exact and mean field methods is obtained for phase insensitive quantities such as averages. The probability density overlap $S_2(t)$ shows very good agreement between the exact and the approximated states.

We conclude from Fig. 3 that the Q/C TDSCF makes significant errors in the phase of the wave function, but the probability density given by $|\Psi|_2$ is actually well represented. The latter is usually of greater practical importance, and the result is therefore encouraging for the approximation. For example, one should expect good predictions using a TDSCF approximation for observables like energies and time of flight spectra in fast direct processes. On the other hand, any measurable quantities which are phase dependent, e.g., spectroscopic line shapes, may not be described accurately by TDSCF. However, we believe that further corrections will improve the method.

Another quantity of interest directly related to the wave function, is the square of the autocorrelation function

$$a(t) = |\langle \Psi(0)|\Psi(t)\rangle|^2. \quad (20)$$

The exact quantum and the TDSCF $a(t)$ values are displayed in Fig. 4. The overall peak positions and heights qualitatively agree, but there are quantitative discrepancies which merit closer attention.

It is evident that at short and intermediate times the exact state decays faster than the TDSCF solution. At longer times the behavior is reversed and the TDSCF decay is the faster one. This is shown by fitting a straight line to the logarithmic fall off of $a(t)$. Assuming

$$a(t) \approx e^{-t/\tau} \quad (21)$$

one gets the unimolecular dissociation lifetimes

$$\tau_{Q/C\,TDSCF} = 0.1055 \text{ ps}, \quad \tau_{\text{exact}} = 0.0869 \text{ ps}. \quad (22)$$

The simulation time was insufficient to calculate τ at long times. Before discussing in details the disagreements between the lifetimes, it should be noticed that the pertinent time scale for the approximation does not exceed a few tenths of a picosecond. In other words, the TDSCF scheme is not expected to provide reliable predictions for times larger that 0.1 or 0.2 ps, at least for the present application model. The fact that $a_{\text{exact}}(t)$ decays faster than $a_{\text{TDSCF}}(t)$ for short (t), and slower for large t, was already noticed in a previous study of vibrational predissociation of $I_2(v)$He.[11] The interpretation we propose is as follows. For short t, the behavior reflects the fact that *TDSCF tends to underestimate correlations between the modes, or equivalently to produce too little energy transfer between the modes.* The time-dependent potentials in the TDSCF equation give rise, of course, to intramolecular energy transfer. However, the spatial details of the correlations between the modes are not described, and in particular, it appears that the energy transfer due to the steep, short-range repulsive interaction between the atoms is not fully represented (or it is too much averaged out) in the SCF approach. The fact that TDSCF often tends to underestimate energy transfer is well known.[5,6,22] The reversal of the behavior is harder to explain, but seems to have the following origin. Because of the "screening" or the "averaging" of the effective potentials the TDSCF wave function can penetrate regions of configuration space that are classically forbidden for the exact Hamiltonian. As the TDSCF errors keep accumulating in time, the unphysical penetration effects increase, and ultimately the TDSCF wave functions significantly occupy parts of space in which the coupling potential is very strong, giving rise to fast decay of the correlation with the initial state. These arguments suggest that the behavior found here and in Ref. 11 should be quite general. Quite obviously, a better choice of coordinates[22] or the inclusion of additional configuration[33] may reduce the deviation of $a_{\text{TDSCF}}(t)$ from $a_{\text{exact}}(t)$ in both time regimes. However, we generally expect "too much separability" and slow decay of correlation with the initial state for TDSCF at short t, and then a too fast decay of the correlation when the TDSCF wave functions have deteriorated beyond a certain level, and have penetrated too strongly into forbidden regions. At the same time, one should note that the TDSCF errors throughout the time domain considered here are not large and the analysis of the deviations from the exact behavior must come second to the fact that the method works well.

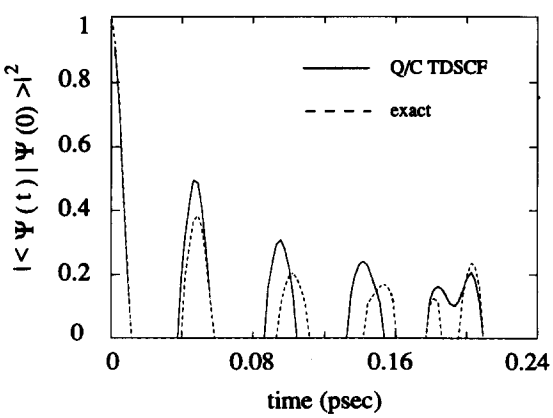

FIG. 4. The autocorrelation function vs time.

The autocorrelation function also yields the vibrational frequency spectrum, by taking the Fourier transform of $\langle \Psi(t)|\Psi(0)\rangle$. For both the exact and the TDSCF approach we obtain a broad peak centered $\approx 780\ \text{cm}^{-1}$, corresponding to the transient frequency of the H atom colliding with the Xe and I atoms. The agreement between the TDSCF and the exact result for this quantity is excellent.

Figure 5 displays the average value of the r coordinate as a function of time. In this figure we also show the result given by the quantum TDSCF approximation, in which both degrees of freedom are treated quantum mechanically [see Eq. (12)].

Up to 0.15 ps, the agreement between the two TDSCF schemes and the exact solution is extremely good. Only at longer times does the quantum TDSCF remain slightly clos-

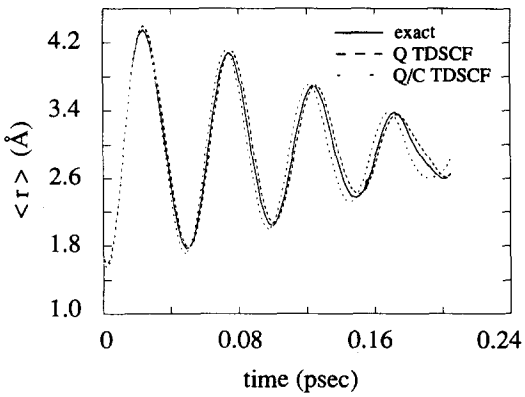

FIG. 5. The average interatomic HI distance as a function of time. Three results are superimposed. Note the small divergence of the Q/C TDSCF at the end.

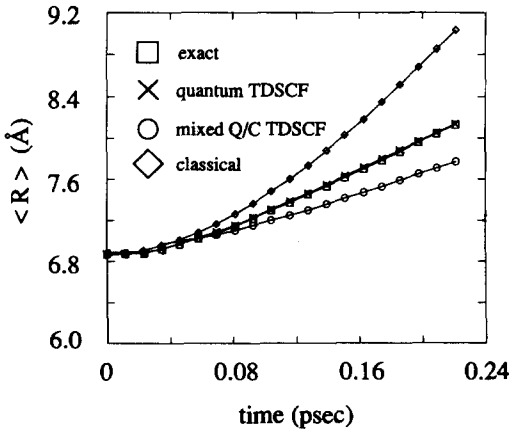

FIG. 7. Time dependence of the average R mode, for all the methods tested in this study. The quantum TDSCF and the exact solution are practically indistinguishable.

er to the exact solution than the mixed Q/C approximation. (Note that the $\langle r \rangle$ value appears to be bounded because we are looking at short times in which the Xe and the I are still relatively near and the H moves in between. At $t \to \infty$, $\langle r \rangle$ will diverge). This behavior is very promising considering the computational advantages of the mixed scheme. A similar effect is evident in Fig. 6 for the time dependency of $\langle p_r \rangle$. Again, phase differences between the curves become accentuated with time. We believe these discrepancies result from the inadequate description of the energy transfer between the modes as a function of time in the TDSCF framework.

Figure 7 presents the average value of the R coordinate vs time. The exact result, the quantum TDSCF, the mixed Q/C TDSCF, and a classical molecular dynamics results are all shown. The agreement between the quantum TDSCF and the exact solution is again excellent, as in the previous cases. However, as time increases, the mixed Q/C TDSCF underestimates the exact result while classical mechanics overestimates it.

The reasons for this are as follows. The increase of $\langle R \rangle$ with time is obviously due to the "hard" collision of the H atom with the Xe and I atoms, in which the high-energy light particle "pushes" the heavier ones. This effect is somewhat stronger in classical than in quantum mechanics, because the quantum H atom is less localized than a classical particle. The partial delocalization of the wave function reduces the pushing effect of the hard collision. Therefore, the $\langle R \rangle$ from full classical dynamics grows faster in time than that of the quantum calculations. In comparing, however, the exact result with Q/C TDSCF, the delocalization for the H atom is about the same in both cases, so another factor becomes decisive: Q/C TDSCF underestimates energy transfer more than quantum TDSCF. The loss of phase coherence in the Q/C TDSCF may be the cause of this, and the decrease of the "pushing efficiency" compared with the exact (and the quantum TDSCF) results. More quantitatively, one can relate the discrepancies between the exact and the approximate schemes to the difference in decay rates described above. Beyond τ one should expect divergence of the TDSCF results from the exact one: after 0.08 ps the deviations from the exact calculation start to increase. Such behavior is particularly evident in Fig. 7, and to a smaller extent in Figs. 5 and 6. Again, one should retain perspective and note that although there is a deviation, even the Q/C TDSCF does fairly well in predicting the time dependence of R and the quantum TDSCF is remarkable in quality.

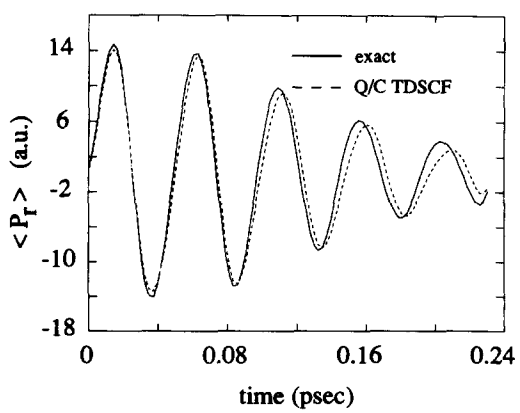

FIG. 6. The average momentum in the r mode as a function of time. As in Fig. 5, the results of the various methods progressively diverge in time.

V. CONCLUSIONS

In this work we presented a comparative study of the photodissociation dynamics of the Xe–HI cluster. A mixed classical/quantal time-dependent self-consistent field approximation was tested against an exact numerical integration of the Schrödinger equation. Considering the enormous computational advantages of the TDSCF and the Q/C TDSCF schemes, the question of their validity is extremely important for they open the way for treating large, realistic systems. The Q/C TDSCF approximation is one of the rare algorithms which saves *both* CPU time and memory storage and this gain should increase with the size of the system. This makes the method particularly appropriate for dealing with quantum many-body problems where exact treatment is out of the question.

The time evolution of the quantum mode in the hybrid treatment reproduces extremely well the corresponding co-

ordinate in the full quantum mechanical solution. This is true not only for average quantities like $\langle r \rangle$ or $\langle p_r \rangle$ *but also for fine details related to the wave function itself.* The good agreement between the autocorrelation functions yields similar transient frequencies and unimolecular dissociation lifetimes for both methods. The description of the energy flow between the quantum and the classical mode is the source of the small, although non-negligible, discrepancies. The message of the present test calculations is therefore very encouraging with respect to the use of TDSCF and Q/C TDSCF, and it seems reasonable to keep applying these methods for an increasing number of problems in molecular dynamics. Again, since the TDSCF approximation is very phase sensitive and limited to short time scale behavior, one should be careful when predicting experimental observables.

Further optimization of the coordinates or inclusion of additional configurations is likely to improve all the results, especially the energy transfer accuracy. This technique has proven successful for improving the static SCF results[22,23] and similar development in TDSCF theory are in their infancy.

Another advantage of the SCF scheme is its intrinsic adaptability to new computer architecture. The parallelization of the SCF algorithm is trivially accomplished by assigning one processor to each degree of freedom. Most of the computation is then carried out independently. Furthermore, both the Fourier transform for the quantum part and the molecular dynamics algorithm for the classical part are easily vectorized and parallelized algorithms.[30–32]

In conclusion, the mixed classical (or semiclassical)/quantal TDSCF approximation appears to be a very promising tool for studying molecular reaction dynamics in a quantum mechanical framework even for systems with many degrees of freedom. The method was found to work well for a major class of processes for which the pertinent time scale is a very short one (subpicosecond). At the same time the results indicate that the quality of the TDSCF approximation deteriorates rapidly in time. This difficulty in the question of how to improve practically the quantum TDSCF and the mixed quantum/classical TDSCF are important issues that merit future research.

ACKNOWLEDGMENTS

The Fritz Haber Research Center at the Hebrew University is supported by the Minerva Gesellschaft für die Forschung, mbH, Munich, Federal Republic of Germany. A. D. H. gratefully acknowledges receipt of a Lady Davis postdoctoral fellowship.

[1] R. Kosloff and D. Kosloff, J. Comp. Phys. **63**, 363 (1986).
[2] R. Kosloff, J. Phys. Chem. **92**, 2087 (1988).
[3] P. A. M. Dirac, Proc. Cambridge Philos. Soc. **26**, 376 (1930).
[4] R. B. Gerber, V. Buch, and M. A. Ratner, in *Intramolecular Dynamics*, edited by J. Jortner and B. Pullman (Reidel, Dordrecht, 1982), p. 171.
[5] R. B. Gerber, V. Buch, and M. A. Ratner, J. Chem. Phys. **77**, 3022 (1982).
[6] G. C. Schatz, V. Buch, M. A. Ratner, and R. B. Gerber, J. Chem. Phys. **79**, 1808 (1983).
[7] G. C. Schatz, Chem. Phys. **24**, 263 (1977).
[8] R. B. Gerber, R. Kosloff, and M. Berman, Comp. Phys. Rep. **5**, 59 (1986).
[9] R. N. Barnet, U. Landman, and A. Nitzan, J. Chem. Phys. **89**, 2242 (1988).
[10] D. Thirmulai, E. J. Bruskin, and B. J. Berne, J.Chem. Phys. **83**, 230 (1985).
[11] R. Bisseling, R. Kosloff, R. B. Gerber, M. A. Ratner, L. Gibson, and C. Cerjan, J. Chem. Phys. **87**, 2760 (1987).
[12] C. Wittig, S. Sharpe, and R. A. Beaudet, Acc. Chem. Res. **21**, 341 (1988).
[13] S. Buelow, G. Radhaknshnan, J. Catanzante, and C. Wittig, J. Chem. Phys. **83**, 44 (1985).
[14] C. Jouvet and B. Soep, Chem. Phys. Lett. **96**, 426 (1983).
[15] N. F. Scherer, L. R. Khundlear, R. B. Bernstein, and A. H. Zewail. J. Chem. Phys. **87**, 1457 (1987).
[16] J. M. Hutson and B. J. Howard, Mol. Phys. **43**, 493 (1981).
[17] G. T. Fraser and A. S. Pine, J. Chem. Phys. **85**, 2502 (1986).
[18] C. Douketis, J. M. Hutson, B. J. Orr, and G. Scoles, Mol. Phys. **52**, 763 (1984).
[19] F. A. Gianturco, A. Palma, P. Villarel, and G. Delgardo-Barrio, Chem. Phys. Lett. **111**, 399 (1984).
[20] R. Alimi and R. B. Gerber, Phys. Rev. Lett. **64**, 1453 (1990).
[21] R. Alimi, R. B. Gerber, and V. A. Apkarian, J. Chem. Phys. **89**, 174 (1989).
[22] R. B. Gerber and M. A. Ratner, Adv. Chem. Phys. **70**, 97 (1988).
[23] (a) Z. Bacic, R. B. Gerber, and M. A. Ratner, J. Phys. Chem. **90**, 3606 (1986); (b) T. R. Horn, R. B. Gerber, and M. A. Ratner, **91**, 1813 (1989).
[24] J. Kucar, H. D. Meyer, and L. S. Cederbaum, Chem. Phys. Lett. **140**, 525 (1987).
[25] G. N. A. Van Veen, K. A. Mohammed, T. Baller, and A. E. De Vries, Chem. Phys. **80**, 113 (1983).
[26] P. Casavecchia, G. He, R. K. Sparks, and Y. T. Lee, J. Chem. Phys. **77**, 1878 (1982).
[27] R. W. Bickes, B. Lantszch, J. P. Toennis, and K. Walascheuski, Discuss. Faraday Soc. **55**, 167 (1973).
[28] H. Tal-Ezer and R. Kosloff, J. Chem. Phys. **81**, 3967 (1984).
[29] R. Kosloff and D. Kosloff, J. Chem. Phys. **79**, 1823 (1983).
[30] P. N. Schwarztrauber, in *Parallel Computations*, edited by G. Rodrigue (Academic, New York, 1982).
[31] H. L. Nguyen, H.Khanmohmmadbaigi, and E. Clementi, J. Comp. Chem. **6**, 634 (1985).
[32] O. Teleman and Bo Jonsson, J. Comp. Chem. **7**, 58 (1986).
[33] A. D. Hammerich, R. Kosloff, and M. A. Ratner, Chem. Phys. Lett. **171**, 97 (1990).
[34] Z. Kotler, A. Nitzan, and R. Kosloff, Chem. Phys. Lett. **153**, 483 (1988).